Characterization of Carrier Concentration and Mobility in n-type SiC Wafers Using Infrared Reflectance Spectroscopy

Katsutoshi Narita[1], Yasuto Hijikata[1], Hiroyuki Yaguchi[1], Sadafumi Yoshida[1,2] and Shinichi Nakashima[2]

[1]*Department of Electrical and Electronic Systems, Faculty of Engineering, Saitama University,*
255 Shimo-Ohkubo, Sakura-ku, Saitama-shi, Saitama 338-8570, Japan
[2]*Power Electronics Research Center, National Institute of Advanced Industrial Science and Technology,*
AIST Tsukuba Central 2, 1-1-1 Umezono, Tsukuba-shi, Ibaraki 305-8568, Japan

We have estimated the free-carrier concentration and drift mobility in n-type 6H-SiC wafers in the carrier concentration range of 10^{17}–10^{19} cm^{-3} from far- and mid-infrared (30–2000 cm^{-1}) reflectance spectra obtained at room temperature. A modified classical dielectric function model was employed for the analysis. We found good agreement between the electrical properties derived from infrared reflectance spectroscopy and those derived from Hall effect measurements. We have demonstrated the spatial mapping of carrier concentration and mobility for commercially produced 2 inch SiC wafers.
[DOI: 10.1143/JJAP.43.5151]

1. Introduction

Silicon carbide (SiC) is a promising material for the fabrication of high-temperature, high-power, and high-frequency electronic devices owing to its advantages of high breakdown electric field, high saturation electron drift velocity, and excellent thermal conductivity. For the practical use of SiC devices, the production of high-quality, large-diameter wafers with uniform electrical properties is indispensable. In order to determine the optimum growth conditions that produce a SiC wafer with a high electrical uniformity and to determine how the electrical properties of the SiC wafer are distributed, it is necessary to characterize the distribution of the electrical properties of the SiC wafer. Previously, to characterize the distribution of the electrical properties of SiC wafers, conductivity mapping was performed.[1,2] However, the mapping of carrier concentration and mobility provides more useful information on the characteristics of wafers than conductivity mapping does, because it determines the distribution of dopant concentration and/or activation of dopants and the crystallinity and/or distribution of crystal defects can be obtained. In order to characterize the distribution of carrier concentration and mobility over SiC wafers, electrical measurement techniques such as Hall effect measurements and capacitance–voltage (C–V) measurements have been widely used. These techniques, however, are disadvantageous device process monitoring tool because they require the formation of electrodes on samples.

Recently, optical measurement techniques such as Raman scattering spectroscopy,[3–6] infrared spectroscopic ellipsometry,[7] optical absorption measurements,[8] and infrared reflectance measurements[9] have been used to characterize the carrier concentration in SiC wafers as nondestructive and contactless methods. It has also been reported that infrared reflectance spectroscopy can characterize the effective electron mass,[10,11] the thickness of homo-epitaxially grown SiC layers,[12–14] and the damage to ion implantation layers.[15–20] We have measured the infrared reflectance spectra of SiC wafers in the spectral range of 600–2000 cm^{-1}, and have shown that infrared reflectance spectroscopy can be used to determine the free-carrier concentration and mobility in SiC wafers by the analysis of the infrared reflectance spectra without destruction or contact.[9] In the case of low-doped SiC wafers ($N \lesssim 10^{18}$ cm^{-3}), however, the spectrum hardly changes in the mid-infrared region including the reststrahlen bands, and it is difficult to characterize the free-carrier concentration and mobility quantitatively from the analysis of this spectrum. To overcome this difficulty, it is necessary to measure the wide spectral region including the wavelength corresponding to the plasma frequency which is determined by the free-carrier concentration. For curve fitting analysis, we had previously used the conventional classical dielectric function (CDF) model.[21] However, it has been reported that the appropriate choice of longitudinal optical (LO) phonon damping constant is necessary to determine the electrical properties of a wide gap semiconductor with an overdamped plasmon system such as SiC by spectroscopic techniques, and a modified classical dielectric function (MDF) is proposed[22] to fulfill this necessity.

In this work, for the reasons mentioned above, we have performed the infrared reflectance measurements in a wide spectral region, i.e., 30–2000 cm^{-1}, for 6H-SiC wafers with a carrier concentration in the range of 10^{17}–10^{19} cm^{-3} at room temperature and have estimated the free-carrier concentrations and mobilities using the MDF model[22] instead of the CDF model. The values obtained from the analysis of the infrared reflectance spectra were compared with those obtained from the Hall effect measurements. Through comparison, we have ascertained that the electrical properties of SiC wafers can be estimated by infrared reflectance spectroscopy with high credibility. Finally, to demonstrate the capability of the method proposed, we have performed the spatial mapping of the carrier concentration and mobility of a commercially produced 2 inch SiC wafer.

2. Experiments

The samples used were single-crystal wafers of n-type (N-doped) 6H-SiC because n-type wafers are utilized mostly for device applications. For the comparison between the electrical properties derived from the infrared reflectance measurements and those from the Hall effect measurements,

wafers with a wide variety of carrier concentrations ranging from 3.7×10^{17} to 2.4×10^{19} cm^{-3} were used. A commercially produced n-type 2 inch 6H-SiC wafer was used for the spatial mapping of carrier concentration and mobility.

The infrared reflectance spectra were measured using two Fourier-transform infrared (FTIR) spectrometers, JASCO FT/IR-VM7 for the far-infrared region (30–600 cm^{-1}) and JASCO FT/IR 670-PLUS for the mid-infrared region (400–2000 cm^{-1}). For the far-infrared reflectance measurements, two light sources (a mercury arc lamp and a nichrome light source), three beam splitters (4-, 12-, and 25-μm-thick Mylar films) and a p-DTGS (pyroelectric deuterated triglycine sulfate) detector were used. For the mid-infrared reflectance measurements, a high-intensity ceramic light source, a KBr beam splitter, and a TGS detector were employed. Each infrared reflectance spectrum was measured at 1 cm^{-1} spectral resolution. The beam diameters were 5 mm and 3 mm for far- and mid-infrared measurements, respectively. The measurements of the (0001) SiC wafers were performed at an approximately normal incidence angle. An Al mirror was used as a reflectance reference.

For the spatial mapping, we employed a micro-FTIR spectrometer (JASCO Irtron IRT-30 infrared microscope), which was equipped with a mercury cadmium telluride (MCT) detector. The diameter of the beam was 0.1 mm. We performed the measurements in the spectral range of 560–2000 cm^{-1} with a spectral resolution of 4 cm^{-1}. We measured at 5 mm intervals over a sample wafer (a total of 120 measurement points).

We cut the SiC wafers to a size of 5×5 mm^2 for the Hall effect measurements using van der Pauw methods. After chemical cleaning, ohmic contacts were fabricated at the corners of each sample by the evaporation of nickel and subsequent heat treatment at 1000°C for 10 min. Infrared reflectance measurements and Hall effect measurements were both carried out at room temperature.

3. Results and Discussion

3.1 Infrared reflectance spectra and their analysis

The dotted lines in Fig. 1 show the typical infrared reflectance spectra of several 6H-SiC wafers of different carrier concentrations at room temperature. The plasma edges and the reststrahlen bands appear in the far-infrared and mid-infrared regions, respectively. For the analysis of infrared reflectance spectra, a number of dielectric function models have been proposed.[21–25] The CDF model, which assumes that the damping constant of the LO phonon is the same as that of the transverse optical (TO) phonon, has been frequently used to analyze the infrared reflectance spectra of not only SiC, but also other polar semiconductors such as GaAs.[26] In SiC, however, the reflectance spectrum is strongly dependent on LO-phonon damping because the plasmon is overdamped and the LO phonon frequency is much higher than the plasma frequency except for heavily doped cases. For these reasons, we have chosen to use the MDF model[22] taking into account the contribution of the TO phonon damping constant and the LO phonon damping constant independently as

$$\varepsilon(\omega) = \varepsilon_\infty \left(\frac{\omega_L^2 - \omega^2 - i\Gamma_L \omega}{\omega_T^2 - \omega^2 - i\Gamma_T \omega} - \frac{\omega_p^2}{\omega(\omega - i\gamma_p)} \right), \quad (1)$$
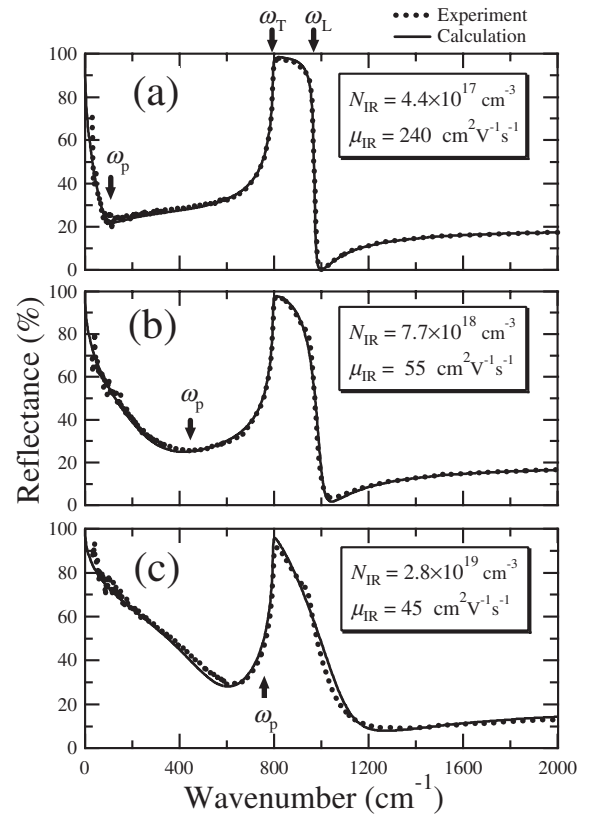
Fig. 1. Infrared reflectance spectra measured for 6H-SiC wafers with various carrier concentrations at room temperature (dotted line). The solid lines show the fitted spectra calculated using the MDF model. The values of carrier concentration and mobility obtained from fitting to the measured infrared reflectance spectra are described in the figure.

where ε_∞ is the optical dielectric constant, ω_T and ω_L are TO and LO phonon frequencies, Γ_T and Γ_L are the TO and LO phonon damping constants, respectively, ω_p is the plasma frequency, and γ_p is the free-carrier damping constant. The first term on the right-hand side of eq. (1) is derived from the Lorentz oscillator model of phonons. The second term is the contribution from free carriers (Drude term). The plasma frequency in the Drude term is given by

$$\omega_p = \left(\frac{Ne^2}{m^* \varepsilon_\infty} \right)^{1/2}, \quad (2)$$

where N, e, m^* are the free-carrier concentration, electron charge, and effective carrier mass, respectively. The free-carrier damping constant γ_p is inversely proportional to the carrier scattering time τ, and therefore the free-carrier drift mobility μ can be derived using the following relation.

$$\mu = \frac{e}{m^* \gamma_p} \quad (3)$$

The reflectivity R from a semi-infinite medium at a normal incidence angle is given by

$$R(\omega) = \frac{(n-1)^2 + k^2}{(n+1)^2 + k^2}, \quad (4)$$

where n and k are the optical constants of the samples.

Carrier concentration and mobility were determined by fitting the experimental infrared reflectance spectrum to the calculated one. To fit the spectra, we used the curve fitting
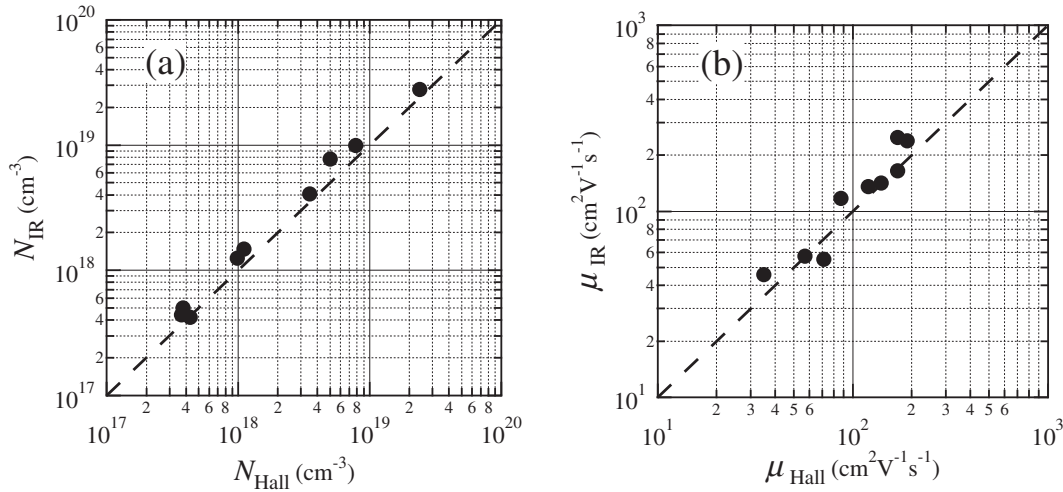
Fig. 2. Comparison of (a) carrier concentration and (b) mobility values obtained from infrared reflectance spectroscopy measurements with those from Hall measurements. The broken line represents the case of complete agreement with each other.

method based on eqs. (1) and (4), in which we adopted ω_p, γ_p, and Γ_L as adjustable parameters. For the values of the other parameters, we employed those obtained from Raman scattering measurement of 6H-SiC;[3] $\varepsilon_\infty = 6.52$, $\omega_T = 797\,cm^{-1}$, $\omega_L = 966.4\,cm^{-1}$, $\Gamma_T = 2\,cm^{-1}$, and $m^* = 0.35m_0$. Since the light is normally incident to the (0001) face of the samples, all these parameters are for the mode vibrating perpendicular to the c-axis (E_1-type mode).

From the curve fitting analysis, we obtained a good fit for each experimental spectrum, which was obtained by measuring nine samples with carrier concentrations in the range of 4×10^{17}–$3 \times 10^{19}\,cm^{-3}$. The solid lines in Fig. 1 show examples of the fitted curves obtained by fitting to the typical infrared reflectance spectra shown as the dotted line in each figure. The free-carrier concentration and drift mobility were derived from the best-fit parameters of ω_p and γ_p using eqs. (2) and (3), mentioned above. The values of free-carrier concentration and mobility obtained are also given in each figure.

As shown in Fig. 1(c), there is a slight discrepancy at approximately $900\,cm^{-1}$ between the spectrum observed and that calculated using the MDF model [eq. (1)]. This discrepancy increases with increasing carrier concentration in the high $10^{19}\,cm^{-3}$ range. For heavily doped SiC crystals, the CDF and MDF models would be inappropriate because the MDF model is derived considering the effects of phonons and plasmons independently. In the case of heavily doped SiC crystals, the plasma frequency is close to the phonon frequency, and the LO phonon and plasmon are strongly coupled. Therefore, though a MDF model can approximately estimate the electrical properties of heavily doped SiC wafers, it is necessary to use another dielectric function model which takes into account the effect of LO phonon-plasmon coupled modes[24,25] to obtain more accurate values.

As the lower limit of the wave number is $30\,cm^{-1}$ in our experiment, we can determine the values of free-carrier concentration to be higher than $1 \times 10^{17}\,cm^{-3}$. In order to characterize samples with a free-carrier concentration less than $10^{17}\,cm^{-3}$, it is necessary to measure infrared reflectance spectra in the region with a wave number less than

$30\,cm^{-1}$, where, however, it is generally difficult to perform measurements with a small beam diameter.

3.2 Comparison with the values derived from Hall effect measurements

In Figs. 2(a) and 2(b), the carrier concentrations and mobilities estimated from the infrared reflectance measurements are plotted against those obtained from the Hall effect measurements, respectively. As the reported Hall scattering factor r_H is approximately unity at room temperature for 6H-SiC,[27,28] we assumed r_H is equal to unity for the calculation. Good agreement was obtained between the electrical properties obtained from the infrared reflectance measurements and those obtained from the Hall effect measurements.

The LO phonon damping constant Γ_L, which is one of the adjustable parameters, varies linearly with carrier concentration. This tendency is in good agreement with the results obtained by Raman scattering spectroscopy,[22] in which, as was explained, the interactions between ionized impurities and LO phonons, and free carriers and LO phonons increase with increasing dopant concentration.

Figure 3 shows the ratios of the free-carrier concentration and mobility estimated from the infrared reflectance measurements to those estimated from the Hall effect measurements (N_{IR}/N_{Hall}, μ_{IR}/μ_{Hall}) for the cases of using the CDF and MDF models for analysis and measurements in the mid-infrared region or far- and mid-infrared region. When the analyses are performed on the spectra in the 600–2000 cm^{-1} range, as shown in Figs. 3(a) and 3(d), there is a noticeable disagreement in the estimated free-carrier concentration and mobility, respectively, between the infrared reflectance measurements and the Hall effect measurements. In particular, this discrepancy is larger in the lower carrier concentration region. These figures also show that the situations cannot be improved by replacing the CDF model with the MDF model. When the region of spectral analysis is extended to the far-infrared region, i.e., 30–2000 cm^{-1}, the agreement between the values obtained from infrared reflectance measurements and those obtained from the Hall measurements is improved significantly in lower carrier concentration region. However, in the case of the CDF
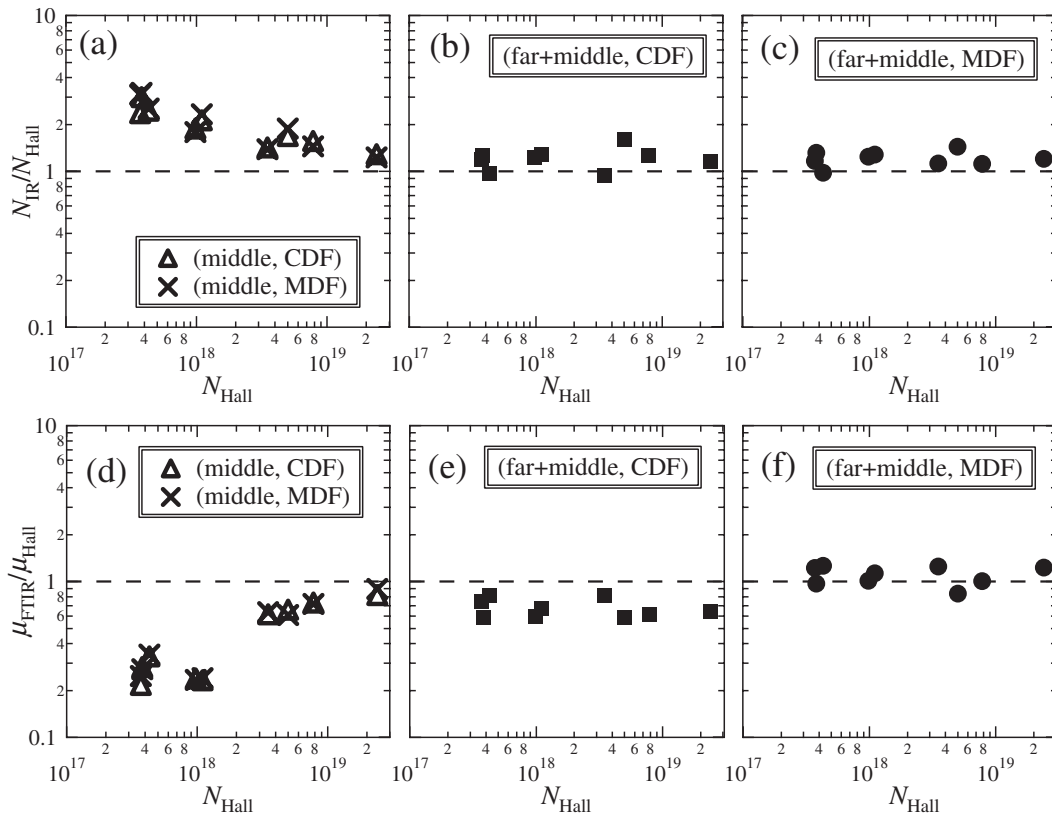
Fig. 3. Ratios of free-carrier concentration and mobility determined from infrared reflectance measurements to those from Hall effect measurements (N_{IR}/N_{Hall} and μ_{IR}/μ_{Hall}) for the cases of using the CDF or MDF model for analysis, and those of measured in the mid-infrared region or far- and mid-infrared region, where the values are plotted against the Hall carrier concentration.

model analysis, the mobilities are estimated to be approximately 0.6 times the values determined by Hall effect measurements. In contrast, when both the far- and mid-infrared region spectra are used and the analysis is performed using the MDF model, both the free-carrier concentration and mobility obtained agree well with those obtained from the Hall measurements. These results indicate that to obtain the carrier concentration and drift mobility from infrared reflectance measurements, it is necessary to measure the spectra over a wide spectral range including the far-infrared spectral region and to use the MDF model for analysis.

3.3 Free-carrier concentration dependence of Hall and drift mobility

In Fig. 4, the drift mobility and Hall mobility of the 6H-SiC wafers are plotted against the determined free-carrier concentration, and against those reported by Karmann *et al.*[29] The Hall mobilities obtained in the present study are a little higher than those determined by Karmann *et al.* in a high-carrier-concentration region. We calculated the drift and Hall mobility at room temperature as functions of dopant concentration following refs. 30–32, assuming that the compensation ratio $N_A/N_D = 0$, and considered five carrier scattering mechanisms (acoustic phonon deformation potential scattering, polar optical phonon scattering, intervalley phonon deformation potential scattering, neutral impurity scattering, and ionized impurity scattering) as in ref. 30. The values of the mobility obtained in this work are lower than those obtained from the theoretical calculations.
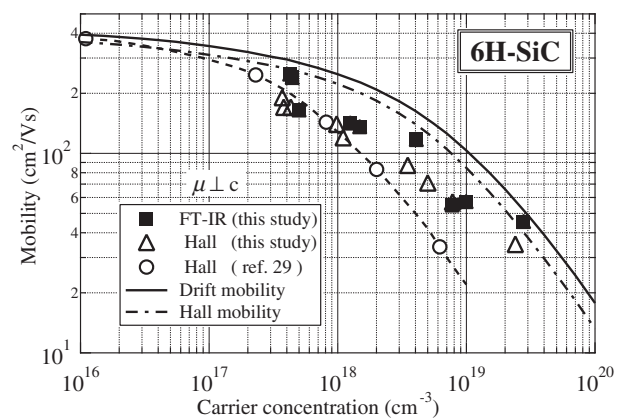
Fig. 4. The variations in drift mobility evaluated from infrared reflectance spectroscopy and Hall mobility measurements plotted against carrier concentration. The reported values of Hall mobility[29] and those calculated theoretically ($N_A/N_D = 0$) following ref. 30 are also shown for comparison.

This result suggests that the compensation ratio is not 0 but approximately 0.2 in this study and a little higher in the case of the data reported by Karmann *et al.*

3.4 Spatial mapping of carrier concentration and mobility over 2 inch SiC wafers

Figure 5 shows an example of the spatial distribution of the free-carrier concentration and mobility of a commercially produced 2 inch 6H-SiC wafer obtained using this
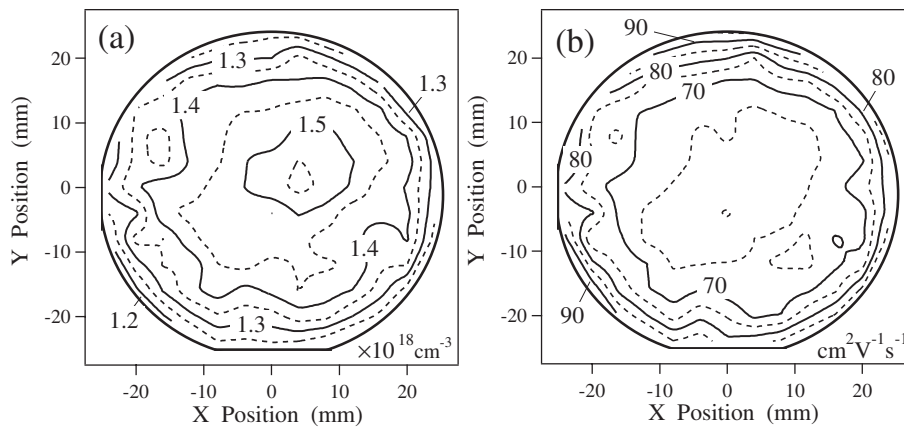
Fig. 5.   Spatial mapping of (a) carrier concentration and (b) mobility in a commercially produced 2 inch SiC wafer.

technique. This measurement technique needs no prior surface treatment, because the native oxide layer thickness and surface roughness are not more than 3 nm and their influence on the reflectance spectra is negligible. The uniformity of the free-carrier concentration and mobility throughout this wafer except for 5 mm from the edge were estimated to be approximately ±9% and ±15%, respectively. The free-carrier concentration mapping shows that the free-carrier concentration in the central region is greater than that in the edge region. On the other hand, the mobility mapping shows the negative correlation of the mobility distribution with that of carrier concentration. When conductivity mapping is used as the method for the mapping of electrical properties of the wafer, it leads to the misleading conclusion that the electrical uniformity over the wafer is approximately ±5% and the wafer is almost uniform, because the conductivity is determined as the product of carrier concentration and mobility. Therefore, the propesed infrared reflectance method is more appropriate for the characterization of the distribution of the electrical properties of SiC wafers.

4.   Conclusions

Far- and mid-infrared reflectance spectra measurements were performed for n-type 6H-SiC single-crystal wafers with different carrier concentrations at room temperature. The free-carrier concentration and mobility were determined from the analysis of the measured spectra using the MDF model. The free-carrier concentration and mobility obtained from the infrared reflectance measurements agree well with the values obtained from Hall effect measurements. These results suggest that infrared reflectance spectroscopy can determine carrier concentration and mobility accurately. Therefore, this method is useful for the characterizzation of the spatial distribution of free-carrier concentration and mobility in SiC wafers as a device process monitoring tool in the carrier concentration range of 10^{17}–10^{19} cm^{-3}. Our results have demonstrated the capability of obtaining the spatial distribution of carrier concentration and mobility in 2 inch SiC wafers using this method.

1) R. Stibal, S. Müller, W. Jantz, G. Pozina, B. Magnusson and A. Ellison: Phys. Status Solidi C **0** (2003) 1013.
2) M. D. Roth, W. E. Carlos, E. R. Glaser, R. Gamble, M. Skowronski, B. V. Shanabrook and D. W. Snyder: to be published in Mater. Sci. Forum.
3) H. Harima, S. Nakashima and T. Uemura: J. Appl. Phys. **78** (1995) 1996.
4) J. C. Burton, L. Sun, M. Pophristic, S. J. Lukacs, F. H. Long, Z. C. Feng and I. T. Ferguson: J. Appl. Phys. **84** (1998) 6268.
5) M. Chafai, A. Jaouhari, A. Torres, R. Antón, E. Martín, J. Jiménez and W. C. Mitchel: J. Appl. Phys. **90** (2001) 5211.
6) H. Yugami, S. Nakashima, A. Mitsuishi, A. Uemonto, K. Furukawa, A. Suzuki and S. Nakajima: J. Appl. Phys. **61** (1987) 354.
7) T. E. Tiwald, J. A. Woollam, S. Zollner, J. Christiansen, R. B. Gregory, T. Wetteroth, S. R. Wilson and A. R. Powell: Phys. Rev. B **60** (1999) 11464.
8) R. Weingärtner, P. J. Wellmann, M. Bickermann, D. Hofmann, T. L. Straubinger and A. Winnacker: Appl. Phys. Lett. **80** (2002) 70.
9) H. Yaguchi, K. Narita, Y. Hijikata, S. Yoshida, S. Nakashima and N. Oyanagi: Mater. Sci. Forum **389–393** (2002) 621.
10) M. A. Il' in, A. A. Kukharskii, E. P. Rashevskaya and V. K. Subashiev: Sov. Phys. -Solid State **13** (1978) 2078.
11) A. V. Mel' nichuk and Yu. A. Pasechnik: Sov. Phys. Solid State **34** (1992) 227.
12) R. T. Holm, P. H. Klein and P. E. R. Nordquist, Jr.: J. Appl. Phys. **60** (1986) 1479.
13) M. F. Macmillan, A. Henry and E. Janzén: J. Electron. Mater. **27** (1998) 300.
14) M. F. Macmillan, P. O. Narfgren, A. Henry and E. Janzén: Mater. Sci. Forum **264–268** (1998) 645.
15) D. Sands, P. H. Key, M. Schlaf, C. D. Walton, C. J. Anthony and M. J. Uren: Mater. Sci. Forum **338–342** (2000) 655.
16) W. Y. Chang, Z. C. Feng, J. Lin, F. Yan and J. H. Zhao: Int. J. Modern Phys. B **16** (2002) 151.
17) Z. C. Feng, F. Yan, W. Y. Chang, J. H. Zhao and J. Lin: Mater. Sci. Forum **389–393** (2002) 647.
18) W. Chang, Z. C. Feng, J. Lin, R. Liu, A. T. S. Wee, K. Tone and J. H. Zhao: Surf. Interface Anal. **33** (2002) 500.
19) J. Camassel, H. Y. Wang, J. Pernot, P. Godignon, N. Mestres and J. Pascual: Mater. Sci. Forum **389–393** (2002) 859.
20) K. Narita, Y. Hijikata, H. Yaguchi, S. Yoshida, J. Senzaki and S. Nakashima: Mater. Sci. Forum **457–460** (2004) 905.
21) E. Neyret, G. Ferro, S. Juillaguet, J. M. Bluet, C. Jaussaud and J. Camassel: Mater. Sci. & Eng. B **61–62** (1999) 253.
22) S. Nakashima and H. Harima: J. Appl. Phys. **95** (2004) 3541.
23) S. Perkowitz: *Optical Characterization of Semiconductors* ed. N. H. March (Academic Press, London, 1993) p. 36.
24) S. Perkowitz and R. T. Thorland: Solid State Commun. **16** (1975)

1093.

25) A. A. Kukharskii: Sov. Phys. Solid State **14** (1972) 1501.

26) R. T. Holm, J. W. Gibson and E. D. Palik: J. Appl. Phys. **48** (1977) 212.

27) G. D. Chen, J. Y. Lin and H. X. Jiang: Appl. Phys. Lett. **68** (1996) 1341.

28) G. Rutsch, R. P. Devaty, W. J. Choyke, D. W. Langer and L. B. Rowland: J. Appl. Phys. **84** (1998) 2062.

29) S. Karmann, W. Suttrop, A. Schöner, M. Schadt, C. Haberstroh, F. Engelbrecht, R. Helbig, G. Pensl, R. Stein and S. Leibenzedar: J. Appl. Phys. **72** (1992) 5437.

30) H. Iwata and K. M. Itoh: J. Appl. Phys. **89** (2001) 6228.

31) H. Iwata, K. M. Itoh and G. Pensl: J. Appl. Phys. **88** (2000) 1956.

32) T. Kinoshita, K. M. Itoh, M. Schadt and G. Pensl: J. Appl. Phys. **85** (1999) 8193.